

93-3241



A93-46775

AIAA 93-3241

**PIV Investigation of an
Aperiodic Forced Mixing Layer**

S. Aissi and L.P. Bernal
University of Michigan
Ann Arbor, MI. 48109-2140

IND 041 03 19 053

AIAA
Shear Flow Conference
July 6-9, 1993 / Orlando, FL

A93-46775-

PIV INVESTIGATION OF AN APERIODIC FORCED MIXING LAYER

S. Aissi* and L.P. Bernal†

The University of Michigan

Ann Arbor, MI. 48109-2140

Abstract

The evolution of large scale vortices produced by acoustical excitation of the mixing layer in an axisymmetric jet was investigated using Particle Image Velocimetry (PIV). The main goal of the investigation is to determine the flow evolution when vortices of different strengths are present in the mixing layer. The flow excitation waveforms used include pure tone waveforms at the most unstable frequency, f_n , and at $0.7 f_n$, as well as an aperiodic waveform consisting of one cycle of frequency $0.7 f_n$ between several cycles of frequency f_n . This later case resulted in the formation of a vortex of larger strength in a stream of vortices formed at the fundamental frequency. The changes in flow evolution associated with these changes in waveform structure are documented with PIV measurements of the velocity and vorticity field.

Introduction

It has long been recognized that turbulent mixing layers can be controlled by the introduction of suitable flow disturbances. The disturbances act to enhance the coherent structures in the flow which in turn produce the desired flow changes. Of particular interest here are the spanwise coherent vortices (or azimuthally coherent in the case of the initial region of a round jet) that control the entrainment process and momentum exchange in the mixing layer.^{1,2} Periodic forcing has often been used in experimental investigations to study the spanwise coherent vortical structures. An enormous volume of work has been done with single frequency forcing such as Zaman & Hussain³, Ho & Huang⁴, Oster & Wygnanski⁵, to name a few. A good review of the subject was conducted by Ho & Huerre⁶. This research has shown that in a perturbed mixing layer the spanwise vortices form at a frequency

determined by, but not necessarily equal to, the frequency of the disturbance.⁴ It was also found that the entire evolution of the flow is locked in phase by the disturbance. Multiple frequency forcing consisting of a fundamental and its subharmonic has also been investigated (see Ng & Bradley⁷; Bradley & Ng⁸; Young & Karlsson⁹), and proved to reduce the vortex path jitter present in single frequency excitation because there is more control over the phase and initial amplitude of the unstable waves.

In the present investigation we consider the evolution of spanwise vortices formed when the disturbance is not periodic. There are significant fundamental changes introduced when the disturbance is not periodic which might have practical implications in flow control. In the "periodic" case all the vortices form with the same strength which results in what could be considered an unstable equilibrium configuration. The subsequent evolution of the flow should be very sensitive to the presence of other disturbances. In contrast, if an aperiodic disturbance is used to produce a stream of vortices of non-equal strength, the resulting configuration is not an equilibrium configuration and therefore might not be as sensitive to the presence of other disturbances. These arguments suggest that the evolution of a vortex of a given strength in an aperiodic mixing layer may not be the same as when the same vortex is produced by periodic disturbances. Forcing of mixing layers with non-periodic disturbances offer a wide range of yet unexplored possibilities in flow control which might prove more efficient to achieve some control objectives.

Figure 1 shows a diagram of a two-dimensional mixing layer including the nomenclature used in this investigation. The experiments were conducted on the mixing layer in the initial region of an axisymmetric jet. Acoustical excitation was used to control the initial vortex formation process. Three cases are studied: 1) Periodic forcing at the most unstable frequency, f_n ; 2) periodic forcing at $0.7 f_n$; and 3) aperiodic forcing consisting of one cycle of frequency $0.7 f_n$ in a stream of cycles of frequency f_n . For each of these cases measurements are reported of the evolution of the velocity and vorticity field obtained using PIV.

* Research Associate, Department of Aerospace Engineering. Member AIAA.

† Associate Professor, Department of Aerospace Engineering. Member AIAA.

Flow Facility and Instrumentation

Flow Apparatus

The experiments were conducted in the near field of an axisymmetric air jet. The jet exit diameter was 7.6 cm. The PIV measurements were conducted within one jet exit diameters downstream of the exit plane of the jet. The flow apparatus was designed to facilitate seeding for the PIV measurements, and to minimize the turbulence intensity at the jet exit. Figure 2 illustrates the air supply system. A high pressure air supply was used. The flow velocity was controlled with a low noise pressure regulator and a variable throat orifice valve. The air flow was fed into an acoustically isolated settling chamber. Downstream of the settling chamber two fine screens, a honeycomb section and a 29 : 1 contraction were used to reduce the turbulence level. At the operating conditions the turbulence level at the jet exit was less than 0.2% and had a broad band frequency spectrum.

The flow was seeded with small particles for flow visualization and for the PIV measurements. The particles were produced by a smoke generator and introduced in the settling chamber. The diameter of the smoke particles at the jet exit was approximately 6 μm as determined from their PIV images. The corresponding Stoke's time and settling velocity were 89 μs and 0.878 mm/s, respectively. In order to measure the velocity of the air entrained by the jet, a coflowing stream seeded with small particles was added to the flow apparatus. The outer stream had a diameter of 33 cm. Honeycomb and foam sections were used to minimize flow disturbances. The air source for the coflowing stream was seeded air from the settling chamber which was diluted with air from a secondary air supply to control the speed and the particle concentration.

PIV Instrumentation

Particle Image Velocimetry (PIV) was used to measure the velocity and vorticity field. The PIV implementation used here is a two step process: First, high resolution photographic images of flow cross-sections on the plane of the main shear are recorded. These images are doubly-exposed images obtained through a rotating mirror to remove the directional ambiguity on the particle displacement. Second, the velocity at all the points of interest is measured using the Young's fringes interrogation technique and the component of the vorticity normal to the image plane is computed.

Illumination and Recording

The illumination and recording system for the PIV measurements consisted of a pulsed laser light source, sheet forming optics, an image shifting system, a photographic camera, and synchronization electronics. Two Nd:YAG lasers were used as the laser light source. Each laser light pulse had a duration of about 9 ns.

Therefore, the particle images were frozen on the PIV images. The output beams of the two Nd:YAG lasers are directed along the same optical axis and passed through a second harmonic generator to obtain a more convenient green laser beam at 532 nm. The lasers were triggered with an elapsed time between them of 11 μs which results in the doubly-exposed image of the particle field.

The sheet forming optics consisted of a combination of two mirrors, a spherical lens, and a cylindrical lens. The two mirrors were used to direct the laser beam in a direction normal to the axis of the jet. A 100 cm focal length spherical lens was used to minimize the laser sheet thickness in the flow. A -25 mm focal length cylindrical lens was used to expand the beam into a sheet. The sheet was positioned along the axis of the jet. At the test section the sheet width was 10 cm, and its thickness was 150 μm approximately.

A large format camera (4" \times 5") with a 135 mm focal length lens was used in this study. The camera was mounted on a heavy Unistrut structure for vibration isolation. The optical magnification was measured directly of the camera screen by placing three rulers in front of the jet and along the plane of the laser sheet. The magnification was determined with a 1% error. The typical magnification used for the PIV measurements was $M = 0.8$. The field of view imaged by the camera was two jet diameters in the flow direction and slightly more than one jet diameter across the flow. The photographic film used in all of the PIV measurements was Kodak 4"x5" Technical Pan 4415 sheets. This film has a fairly high resolution (300 lines/mm) and its contrast and granularity can be adjusted by using appropriate processing solutions and temperatures. The film was developed for 6 minutes in Kodak D-19 developer, resulting in an ASA-200 exposure and a 2.4 contrast index, which are close to the maximum attainable levels for this type of film.

A systematic study was conducted to determine the optimum seeding concentration for the PIV measurements. The main criteria in this study was to obtain good fringe quality for the interrogation system. An optimum value of 60 particles/mm³ was obtained for the average particle concentration in the jet flow field. In the coflowing stream, a particle concentration of about 35 particles/mm³ was used, which is about half of the concentration in the jet flow.

The PIV illumination technique used here has two inherent limitations. First, it is not possible to distinguish the order in which the particle images on a pair were obtained, thus a 180 degree directional ambiguity exists. Secondly, fringes are not formed when the particle displacements are smaller than the particle diameter. To resolve the ambiguity of the velocity vector and to improve the resolution in the low velocity range, an image shifting (or, velocity biasing) technique was employed. The most commonly used methods are a rotating mirror¹⁰ and electro-optical devices.¹¹ The image shifting technique

consists on adding a known bias velocity to the actual flow velocity during the photographic recording process. This additional bias velocity is subtracted from the velocities measured after the interrogation.

In this study, the rotating mirror technique was used because of its simplicity. The rotating mirror system was positioned in front of the camera lens and mounted to the same aluminium plate as the camera body. Sensors attached to the rotating mirror were used to 1) trigger the laser at the proper angular position of the mirror, 2) measure the instantaneous angular velocity of the mirror to determine the bias velocity, and 3) provide a suitable synchronization signal for the flow excitation system. The synchronization signal was used to adjust the elapsed time between the initiation of the excitation waveform and the laser trigger. The phase of the excitation signal at the time of the PIV measurement was measured with an accuracy of 1 μ s. In these experiments the mirror angular velocity was 300 rpm. The corresponding bias velocity was 10 m/s in the cross-flow direction.

Interrogation System

The PIV images were analyzed using the Young's fringe method. The procedure used in these measurements is described by Kwon.¹² The PIV photographic negative was mounted on a glass surface inside a holding frame which was attached to a precision computer-controlled traverse system. A 15 mW HeNe laser beam was used to illuminate a small circular area on the negative with an effective diameter of about 1 mm. The interference of scattered light off the particle images produced Young's interference fringes. A 864 mm spherical lens was used to focus the undiffracted laser beam to a waist where it was removed by a beam stop. The fringe pattern on this plane was imaged with a video camera using a 135 mm lens and a 305 mm lens. Neutral density filters and a polarizer were used to control the image intensity on the video camera. The fringe image was analyzed using the technique described by Kwon.¹²

To compute the local velocities, the fringe spacing as well as their orientation were measured. The fringes have an orientation which is perpendicular to the direction of the local displacement of the particles and a spacing proportional to the particle displacement. The local velocities are obtained using the relation

$$u_p = \lambda_i f / M d_f \Delta t \quad (1)$$

where u_p is the magnitude of the velocity, λ_i is the wavelength of the HeNe laser, f is the focal length of the interrogation lens, d_f is the measured fringe spacing, M is the magnification of the optical recording system (≈ 0.8), and Δt is the elapsed time between exposures ($\approx 11\mu$ s). The photographic negative was interrogated in a rectangular grid using a grid spacing of 1 mm which corresponds to a grid resolution of 1.25 mm in the flow.

From the PIV data, vector plots were obtained to show the overall instantaneous flow pattern. In addition to the velocity field measurements, the component of the vorticity normal to the plane of the measurement was obtained using Stokes' theorem

$$\omega_z = \lim_{A \rightarrow 0} \left(\frac{\Gamma}{A} \right), \quad (2)$$

where the circulation Γ was computed around a closed contour about each point using the definition

$$\Gamma = \oint \vec{u} \cdot d\vec{\ell}. \quad (3)$$

The trapezoidal rule was used to calculate this line integral.

PIV measurements in the potential core of the jet were used to evaluate the uncertainty of the measurements. The uncertainty of the velocity measurements was less than 1%. The RMS value of the out-of-plane vorticity fluctuation was found to be 88.977 s⁻¹. This corresponds to an error of less than 10% of the maximum measured vorticity.

Flow Excitation

Various techniques have been used in the past to introduce disturbances in mixing layers; among these are an oscillating flap,⁵ a vibrating ribbon,¹³ a reciprocating piston,¹⁴ and a loudspeaker.^{3,15} Of these a loudspeaker was chosen for this investigation because it is easy to implement and test. An arrangement similar to Becker & Massaro¹⁶ was used in the present work. The loudspeaker was placed on one side of the jet nozzle at 45 degrees relative to the flow direction and 60 cm away. The loudspeaker was driven by a programmable multifunction synthesizer and a variable-gain power amplifier. The acoustic field generated by this system was tested for uniformity in the mixing layer region using a microphone. The signal from the loudspeaker was recorded on a digital storage oscilloscope. It was found to be uniform over a region covering at least 3 jet diameters downstream of the jet exit.

Since the mixing layer is very sensitive to the frequency of the forcing signal, and since all of the forcing signals used in our study involve ratios or combinations of the fundamental frequency, f_n , the fundamental frequency had to be measured with a high degree of accuracy. The flow speed was first set at a pre-determined value using a pitot tube placed at the center of the jet exit and a precision manometer. The fundamental frequency was measured in three ways. The first two methods involved hot film measurements at the jet exit. In the first method the output of the hot film anemometer was monitored using a digital storage oscilloscope. The measured period of this signal gives f_n . For the second method, a transient digitizer was used to digitize the output of the hot film anemometer and to determine the power spectrum of the velocity signal. The fundamental frequency, f_n , was easily obtained from the power spectrum. The third method for obtaining f_n was

to use the results of the stability theory. The Strouhal number St_n of the most unstable disturbance^{17,18} based on a hyperbolic tangent mean velocity profile is

$$St_n = \frac{f_n \theta_0}{u_c} = 0.032, \quad (4)$$

where θ_0 is the initial momentum thickness of the laminar mixing layer and u_c is the average speed across the mixing layer. The initial momentum thickness was measured using the hot film anemometer system. Typically, the first and second methods used to determine the fundamental frequency gave similar results, while the third method was off by about 20%. This difference is in agreement with the results of Sato¹⁹, and Zaman & Hussain,³ who also found the same discrepancies between the value of the natural roll-up frequency and the larger value of the most unstable frequency.

A flow visualization study was performed to select a forcing amplitude which produced the least vortex "jitter" in the mixing layer. Flow visualization pictures were obtained using the optical system described earlier while varying the gain of the power amplifier in small increments. The forcing level corresponding to the least jitter in the roll up of the large-scale vortices formed at the fundamental frequency was chosen for all the measurements.

For the present investigation, the purpose of the acoustic excitation system was to introduce a known disturbance and to provide a phase reference for the PIV measurements. Two types of forcing waveforms were used. First, a forcing waveform consisting of a pure sine wave pulsed for twenty periods at the desired frequency was used to form vortices of the equal strength. The other type of excitation waveform consisted of eight periods of the fundamental frequency, f_n , followed by one period of a frequency, $0.7 f_n$, as illustrated in Figure 3. Three of these sequences were generated in succession for each test.

Additional details on the flow facility and instrumentation can be found in reference 20.

Results

The results presented below were obtained for a jet speed $u_e = 7$ m/s, and coflowing stream speed of about 0.6 m/s. Therefore the velocity ratio across the mixing layer was approximately 0.086. The corresponding Reynolds numbers based on the jet diameter ($D = 7.62$ cm) and the initial momentum thickness ($\theta_0 = 0.4739$ mm) were $Re_D = 3.56 \times 10^4$ and $Re_{\theta_0} = 222$, respectively. The measurements covered a region $x \leq D$. In this region, the effect of the cross-stream curvature on the dynamics of the mixing layer of the circular jet are small,²¹ which allows comparison with plane mixing layers. In this region, the appropriate length scale is the initial momentum thickness, θ_0 , or equivalently the initial instability wavelength u_c/f_n , where

u_c is convection speed of the large scale vortices (≈ 3.8 m/s). At these flow conditions the measured natural frequency was $f_n = 208$ Hz. ($\tau_n = 4.8$ ms)

One important advantage of PIV is that it provides a flow visualization image, a velocity map and a vorticity map all obtained at the same instant in time. This is illustrated in Figure 3 which shows the PIV image (Figure 3a) obtained at a forcing frequency of $0.7 f_n = 146$ Hz, the measured velocity field in the laboratory frame of reference (Figure 3b), the velocity field in the frame of reference moving with the large scale vortices (Figure 3c), and the vorticity field (Figure 3d). The PIV image provides an excellent visualization of the flow. In this case it reveals two vortices in the process of amalgamation in the center of the image and an unusually small vortex downstream of the vortices undergoing amalgamation. The velocity vector plot in the laboratory frame of reference, Figure 3b, shows complex velocity patterns with reverse flow regions in the low speed side of the mixing layer. The velocity vector plot in a frame of reference moving with the large scale vortices, Figure 3c, reveals details of the flow structure around the vortices. Points of high circulation associated with concentrated vorticity are easily identified on this vector plot. Also saddle points can be identified on this plot. Finally, the vorticity plot in Figure 3d shows the regions of high vorticity, which correspond well with the region of high circulation in the velocity vector plots.

The results for a mixing layer forced at the natural frequency, $f_n = 208$ Hz, are shown in Figures 4 to 6. Figure 4 shows the flow visualization PIV images obtained at three different phases of the forcing signal. Figure 5 are velocity vector plots in a frame of reference of moving with the vortices. Figure 6 are the corresponding vorticity contour plots. It should be noted that the flow pictures cover a flow region larger than the velocity and vorticity data. The flow evolution provided by these data is in good agreement with earlier work.⁶ A thin vorticity containing region near the lip of the jet roll up into well defined vortices, which are then convected downstream. The flow pictures also shows that the vortices undergo pairing farther downstream.

The strength and size of the roll-up vortices can be determined from the vorticity measurements. For our purpose here we define a vortex as the region enclosed by the vorticity contour of value -500 s^{-1} . The circulation of the vortices was measured to be $-0.131 \pm 0.024 \text{ m}^2/\text{s}$ which gives a normalized value $\Gamma/u_c \lambda = 1.03$ in good agreement with the expected value of 1. Another important parameter is the maximum vorticity in the core of the large scale vortices. For the vortices in this sequence we find $\omega_z f_n = -12 \pm 1$. These values are a factor of two larger than the values measured using phase averaging techniques.^{3,22}

The results for a mixing layer forced at a frequency, $f_s = 0.7 f_n = 146$ Hz, are shown in Figures 7 to 9. Figure 7 shows the flow visualization PIV images obtained at three different phases of the forcing signal as indicated. Figure 8

are velocity vector plots in a frame of reference of moving with the vortices. Figure 9 are the corresponding vorticity contour plots. In this case the flow evolution is somewhat different than for the natural frequency. The flow pictures suggest that the shear layer rolls-up into small vortices, smaller than the value determined from the forcing frequency. However the velocity and vorticity plots show that vorticity is not very concentrated in this region. A well defined vortex forms farther downstream at the forcing frequency. The flow visualization pictures also suggest that this vortex amalgamates at the downstream end of the picture.

The circulation of the vortices was also measured in this case. However there are few well formed vortices in the sequence. For the well formed vortex at the center of the image at $\phi = 0.44 \tau_s$ the circulation is $-0.1624 \text{ m}^2/\text{s}$, which corresponds to $\Gamma/u_e \lambda = 0.97$ also in good agreement with the expected value of 1. The normalized value of the maximum vorticity was found to be $\omega_z f_s = -13 \pm 3$ also much larger than previously reported.

The results for a mixing layer forced with a waveform consisting of one cycle at frequency $f_s = 146 \text{ Hz}$ combined with several cycles of frequency $f_n = 208 \text{ Hz}$, are shown in Figures 10 to 12. Figure 10 shows the flow visualization PIV images obtained at five different phases of the forcing signal as indicated. Figure 11 are velocity vector plots in a frame of reference of moving with the vortices. Figure 12 are the corresponding vorticity contour plots. In the first two images of the sequence the vortex formed at frequency f_s is within the field of view. However, all the data suggests that the vortex is not well developed. The vorticity contours show an elongated concentration of vorticity at the location of this vortex. This vortex appears to reach a more well developed state in the third image of the sequence. The vortex is now located at the downstream end of the image. It is interesting to compare this result with the evolution for periodic forcing at f_s discussed earlier which show that at the same downstream location the vortex was undergoing amalgamation. At later times in the evolution, the vortices within the field of view are formed at frequency f_n . These data show that their evolution is essentially the same as for the periodic forcing at f_n . In particular amalgamation occurs at the same downstream location.

Conclusions

The evolution of large scale vortices in the mixing layer region of a round jet was investigated experimentally. Periodic and aperiodic forcing was used to study the flow using PIV measurements. The main conclusions of this study are:

- The general evolution and qualitative features of large scale structures produced by periodic forcing are in good agreement with the results of previous investigations.

- The measured values of the normalized maximum spanwise vorticity in the core of the large scale vortices ($\omega_z f \approx 12-13$) are significantly larger than previously reported.
- The circulation of vortices in the mixing layer was measured and found to be in good agreement with the estimate $\Gamma/u_e \lambda \approx 1$.
- The evolution of a vortex of large strength is significantly delayed by the presence of vortices formed at the natural frequency.
- The evolution of vortices formed at the natural frequency are not influenced by the presence of a larger strength vortex.

Acknowledgments

The authors will like to acknowledge the financial support of *Ford Motor Co.* for the development of the PIV interrogation software.

References

1. BROWN, G.L. & ROSHKO, A. 1961 On density effects and large structure in turbulent mixing layers. *Journal of Fluid Mechanics* **64**, 775-816.
2. WINANT, C.D. & BROWAND, F.K. 1974 Vortex pairing, the mechanism of turbulent mixing-layer growth at moderate Reynolds numbers. *Journal of Fluid Mechanics* **63**, 237-255.
3. ZAMAN, K.B.M.Q. & HUSSAIN, A.K.M.F. 1980b Turbulence suppression in free shear flows by controlled excitation. *Journal of Fluid Mechanics* **103**, 133-159.
4. HO, C.M. & HUANG, L.S. 1982 Subharmonics and vortex merging in mixing layers. *Journal of Fluid Mechanics* **119**, 443-473.
5. OSTER, D. & WYGNANSKI, I. 1982 The forced mixing layer between parallel streams. *Journal of Fluid Mechanics* **123**, 91-130.
6. HO, C.M. & HUERRE, P. 1984 Perturbed free shear layer. *Annual Review of Fluid Mechanics* **16**, 365-424.
7. NG, T.T. & BRADLEY, T.A. 1988 Effect of multifrequency forcing on the near-field development of a jet. *AIAA Journal* **26**.
8. BRADLEY, T.A. & NG, T.T. 1989 Phase-locking in a jet forced with two frequencies. *Experiments in Fluids* **7**, 38-48.
9. YANG, Z. & KARLSSON, S.K.F. 1991 Evolution of coherent structures in a plane shear layer. *Physics of Fluids A* **3**, 2207-2219.

10. ADRIAN, R.J. 1986 Image shifting technique to resolve directional ambiguity in double-pulsed velocimetry. *Applied Optics* **25**, 3855-3858.
11. LANDRETH, C.C. 1986 Two-dimensional measurement of complex flows using pulsed laser velocimetry with directional resolution. M.S. thesis, University of Illinois at Urbana-Champaign.
12. KWON, J.T. 1989 Experimental study of vortex ring interaction with a free surface. Ph.D. thesis, The University of Michigan.
13. MENSING, P. 1981 Einfluss kontinuierlicher Störungen auf eine ebene turbulente Scherschicht. Dissertation Hermann-Fottinger-Institut, TU Berlin.
14. DISIMILE, P.J. 1986 Phase averaged transverse vorticity measurements in an excited, two-dimensional mixing layer. *AIAA Journal* **24**, 1621-1627.
15. FREYMOUTH, P. 1966 On transition in a separated laminar boundary layer. *Journal of Fluid Mechanics* **25**, 683-703.
16. BECKER, H.A. & MASSARO, T.A. 1968 Vortex evolution in a round jet. *Journal of Fluid Mechanics* **31**, 435-448.
17. MICHALKE, A. 1965a Vortex formation in a free boundary layer according to stability theory. *Journal of Fluid Mechanics* **22**, 371-383.
18. MICHALKE, A. 1965b On spatially growing disturbances in an inviscid shear layer. *Journal of Fluid Mechanics* **23**, 521-544.
19. SATO, H. 1960 The stability and transition of a two-dimensional jet. *Journal of Fluid Mechanics* **7**, 53-80.
20. AISSI, S. 1992 Evolution of the Large-Scale Vortices in Turbulent Mixing-Layers. Ph.D. Thesis, University of Michigan.
21. HUSSAIN, A.K.M.F. 1986 Coherent structures and turbulence. *Journal of Fluid Mechanics* **173**, 303-356.
22. BROWAND, F.K. & WEIDMAN, J. 1976 Large scales in the developing mixing layer. *Journal of Fluid Mechanics* **76**, 127-144.

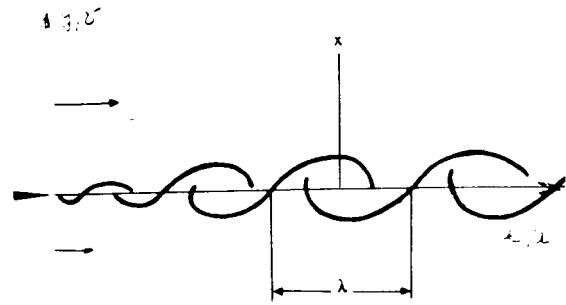


Figure 1. Schematic diagram of the mixing layer.

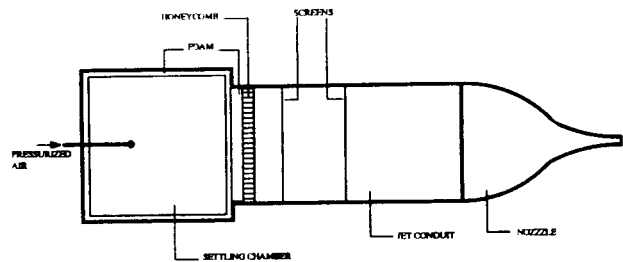


Figure 2. Schematic diagram of jet flow facility.

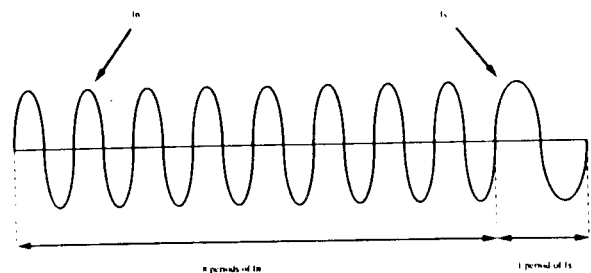
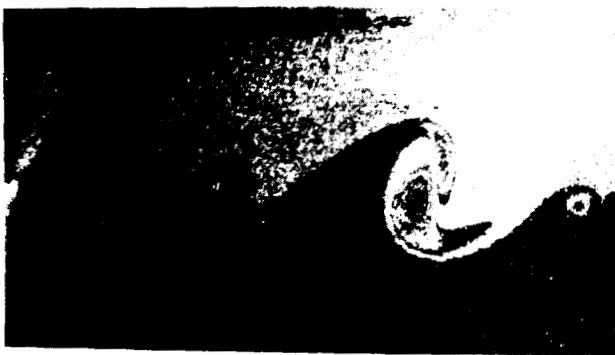
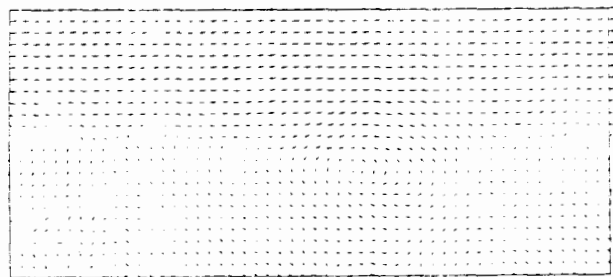


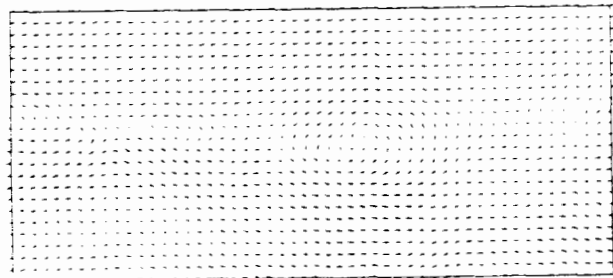
Figure 3. Aperiodic waveform used to produce a vortex of frequency f_s between eight vortices of frequency f_n .



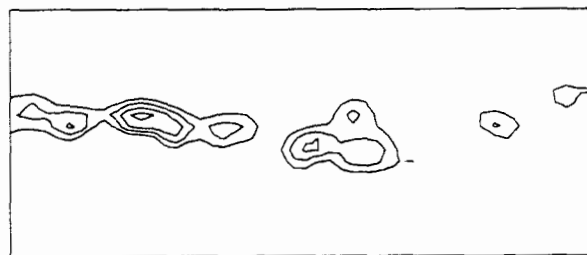
(a)



(b)

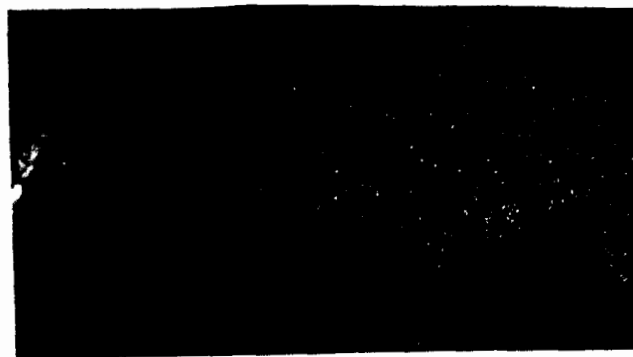


(c)



(d)

Figure 4. PIV data for a forcing frequency $f_s = 146$, at a phase lag $\phi = 0.44 \tau_n$. (a) PIV image, (b) Velocity vector plot in a stationary frame of reference, (c) Velocity vector plot in a frame of reference moving with the vortices, and (d) Vorticity contour plot (contour level plotted -1200, -1600, -2000, -2400, -2800 sec^{-1})



(a)

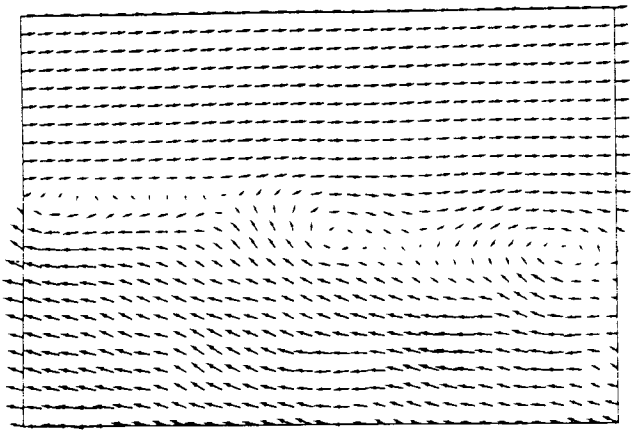


(b)

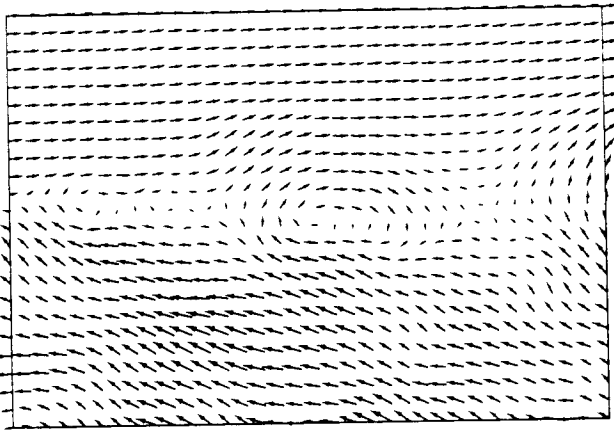


(c)

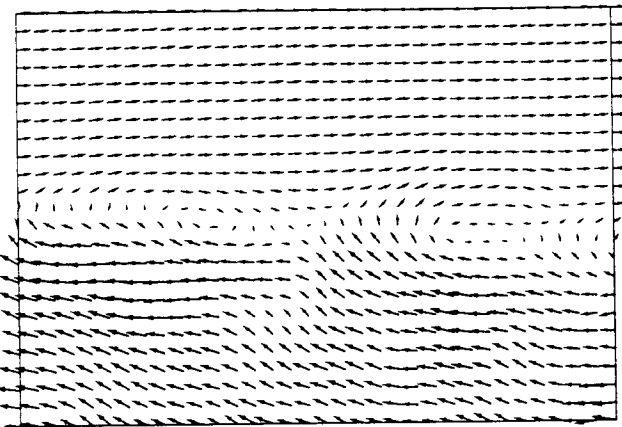
Figure 5. PIV flow pictures for $f_n = 208 \text{ Hz}$. (a) $\phi = 0.24 \tau_n$, (b) $\phi = 0.49 \tau_n$, (c) $\phi = 0.89 \tau_n$.



(a)

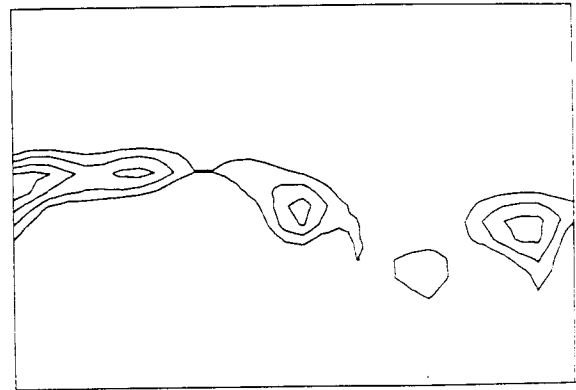


(b)

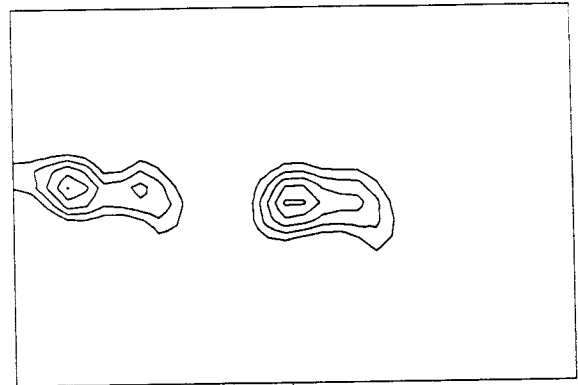


(c)

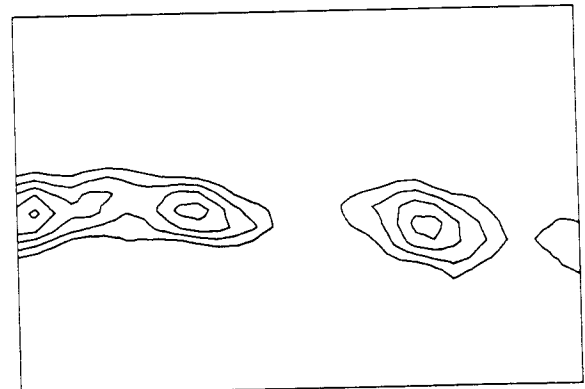
Figure 6. Velocity vector plot in a frame of reference moving with the vortices for $f_n = 208$ Hz. (a) $\phi = 0.24 \tau_n$, (b) $\phi = 0.49 \tau_n$, (c) $\phi = 0.89 \tau_n$.



(a)



(b)



(c)

Figure 7. Vorticity contour plot for $f_n = 208$ Hz. (a) $\phi = 0.24 \tau_n$, (b) $\phi = 0.49 \tau_n$, (c) $\phi = 0.89 \tau_n$. Contour levels same as in Figure 4



(a)

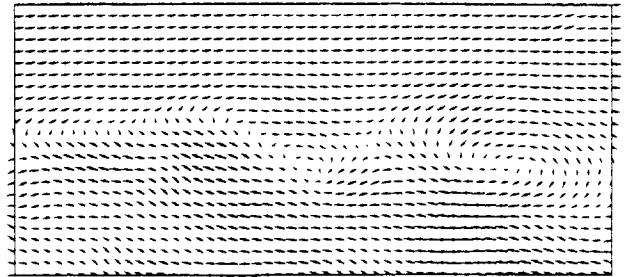


(b)

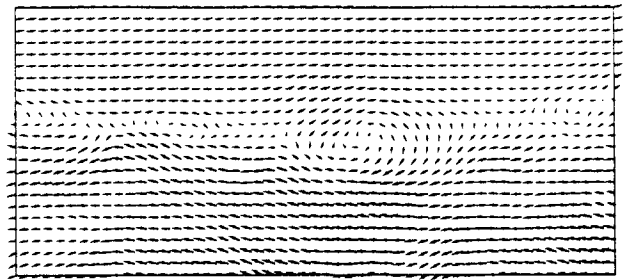


(c)

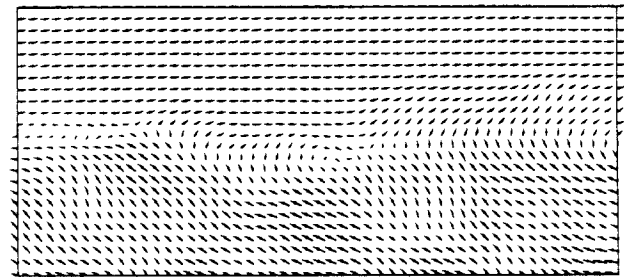
Figure 8. PIV flow pictures for $f_s = 146$ Hz. (a) $\phi = 0.03 \tau_s$, (b) $\phi = 0.44 \tau_s$, (c) $\phi = 0.86 \tau_s$.



(a)



(b)



(c)

Figure 9. Velocity vector plot in a frame of reference moving with the vortices for $f_s = 146$ Hz. (a) $\phi = 0.03 \tau_s$, (b) $\phi = 0.44 \tau_s$, (c) $\phi = 0.86 \tau_s$.

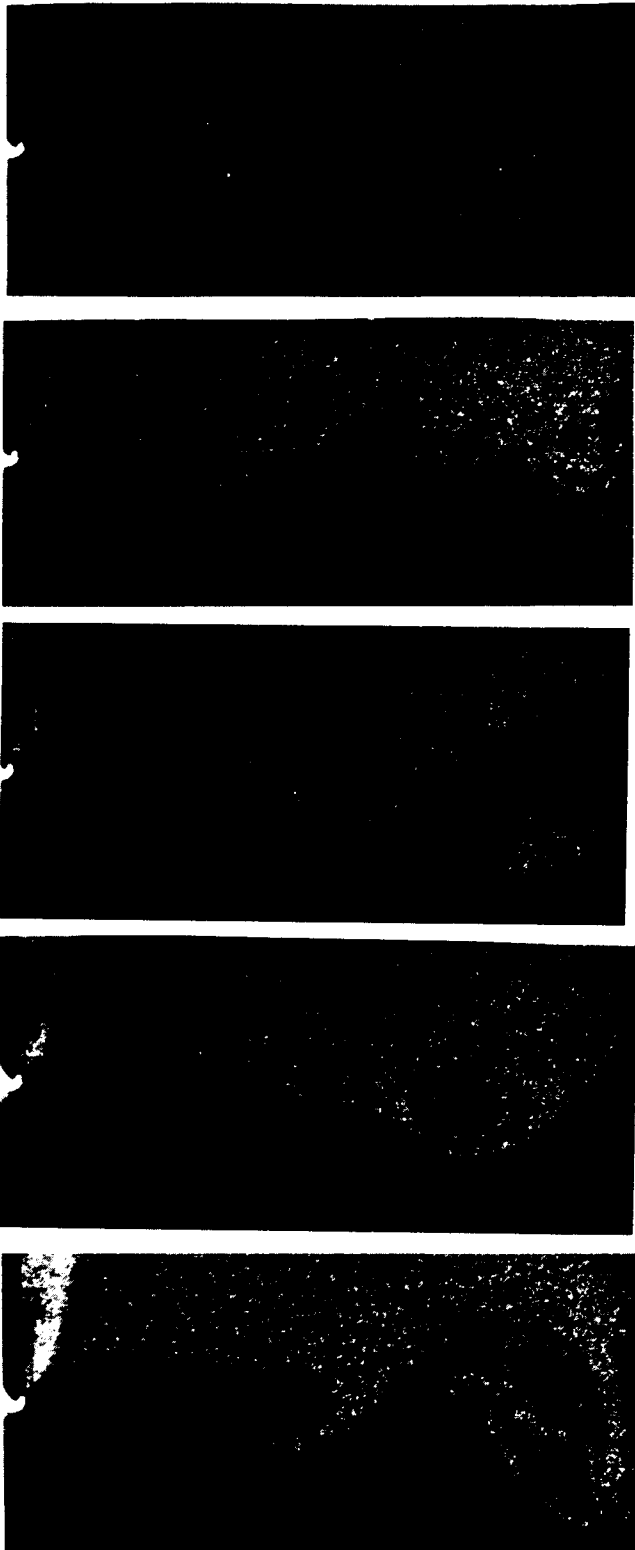
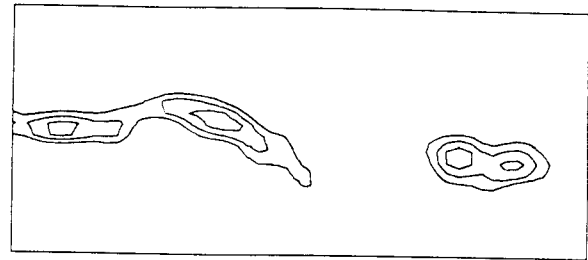
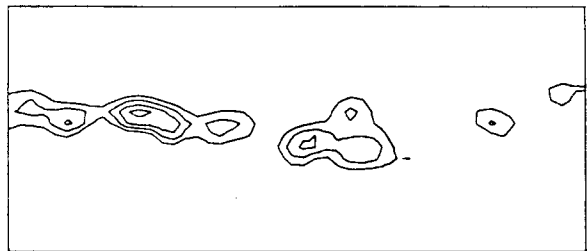


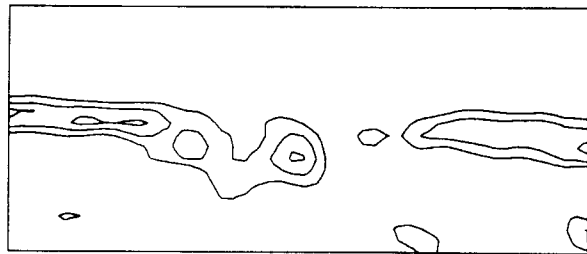
Figure 11. PIV flow pictures for aperiodic forcing. Phase relative to the cycle of frequency f_s , from top to bottom: 9.9, 13.1, 16.6, 20.2, 23.5 ms.



(a)



(b)



(c)

Figure 10. Vorticity contour plot for $f_s = 146$ Hz. (a) $\phi = 0.03 \tau_s$, (b) $\phi = 0.44 \tau_s$, (c) $\phi = 0.86 \tau_s$. Contour levels same as in Figure 4.

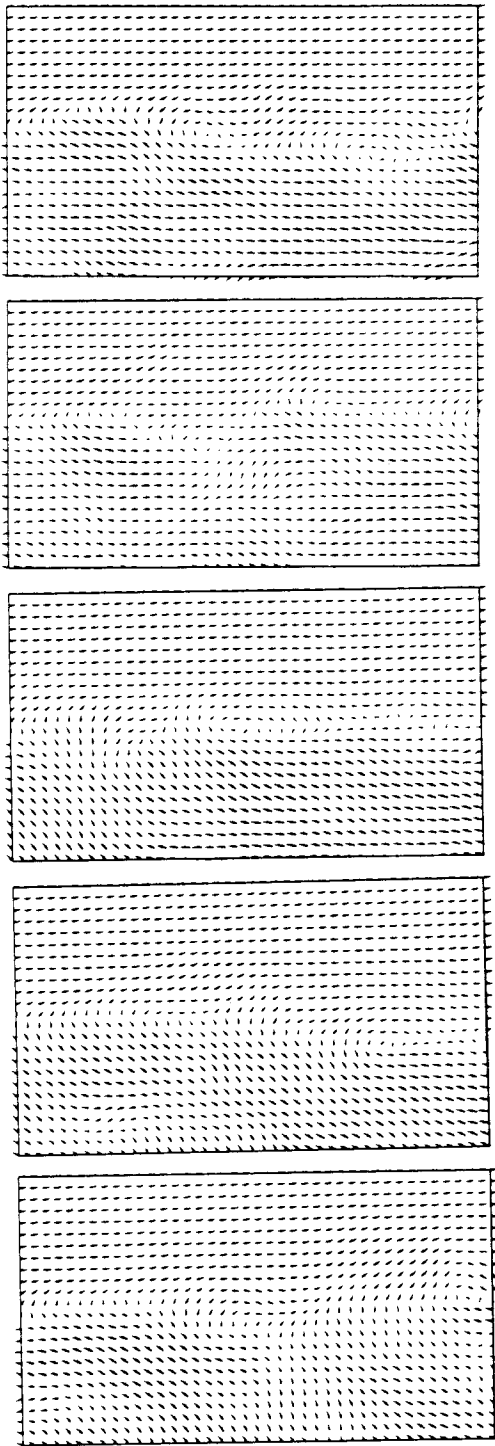


Figure 12. Velocity vector plot in a frame of reference moving with the vortices for aperiodic forcing. Same conditions as in Figure 11.

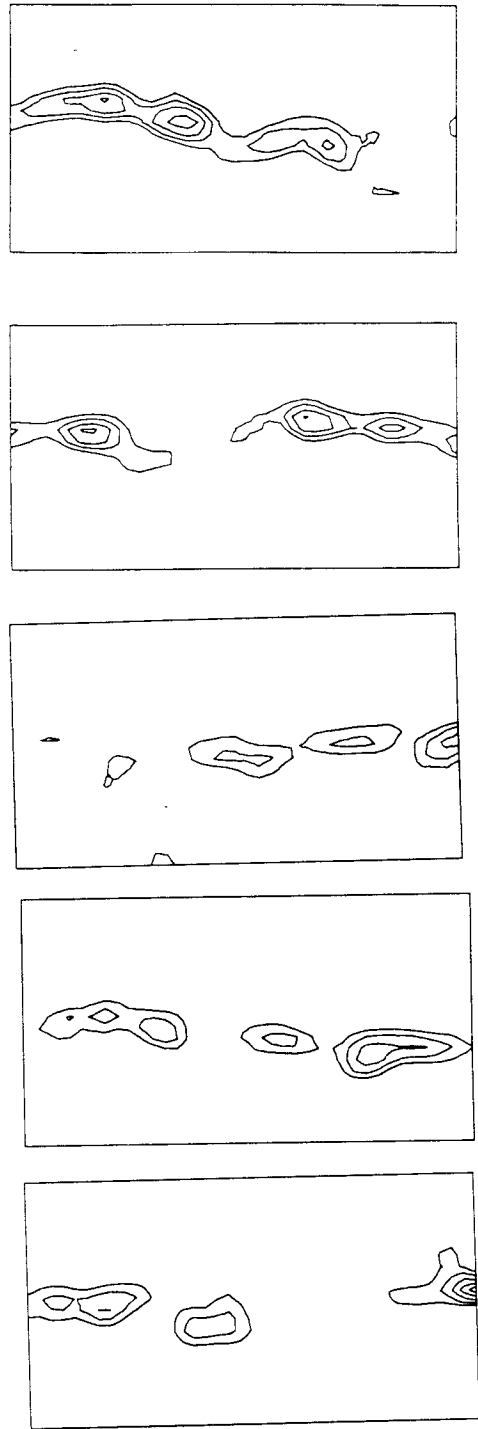


Figure 13. Vorticity contour plot for aperiodic forcing. Same conditions as in Figure 11.